Electronic Supplementary Material (ESI) for ChemComm.

Supporting information for

In situ creation of multi-metallic species inside porous silicate materials with tunable catalytic properties

Yang-Yang Liu, Guo-Peng Zhan and Chuan-De Wu*

State Key Laboratory of Silicon Materials, Department of Chemistry, Zhejiang University, Hangzhou, 310027, P. R. China

Materials

Nickel perchlorate hexahydrate (99%), cobalt perchlorate hexahydrate (99%), gadolinium chloride hexahydrate (99%), sodium benzoate (99%), hydroxymethylpyridine (98%, hmp-H), triethylamine (99.5%), tetraethyl orthosilicate (99%, TEOS) and halogenated nitrobenzenes (99%) were supplied by Saan Chemical Technology Co., Ltd (Shanghai, China). Isopropanol (99.7%) was supplied by Sinopharm Chemical Reagent Co. Ltd (China). High purity hydrogen (99.999%) was supplied by Hangzhou Jingong Materials Co. Ltd (China). All reagents used in this work are of analytical grade, which were directly used without further purification.

Preparation of PMS-11

PMS-11 was prepared by employing sol−gel method. Sodium benzoate (2.5 mmol), $Ni(ClO_4)_2 \cdot 6H_2O$ (0.5 mmol) and $Co(ClO_4)_2 \cdot 6H_2O$ (0.5 mmol) were dissolved in 30 mL of methanol under stirring. $GdCl_3 \cdot 6H_2O$ (1 mmol), Et_3N (2 mmol) and hmp-H (2 mmol) were successively added into the mixture under stirring. The mixture was further reacted at room temperature for 4 h, resulting a coordination complex $[NiCoGd_2(hmp)_4(PhCO_2)_5(ROH)_2](ClO_4)$ (abbreviated as $[NiCoGd_2]$). Subsequently, a TEOS solution (4 mL TEOS, 2 mL H_2O and 8 mL MeOH) was dropwise added into the $[NiCoGd_2]$ solution, which was stirred at room temperature for 30 min. The resulting sol-gel was transferred into a Teflon-lined autoclave, which was reacted at 160 °C for 48 h. The resulting brown solid was dried in oven at 60 °C for 2 h, which was annealed at different temperatures (400, 500, 600, 700 and 800 °C) under N_2 atmosphere for 2 h.

Catalyst characterization

Transmission electron microscopy (TEM, HT7700 and JEM 2100F) and scanning electron microscope (SEM, Hitachi S-4800) were used to characterize the morphology of PMS-11. Powder X-ray diffraction (PXRD) data were recorded on a RIGAKU D/MAX 2550/PC for Cu Kα radiation (λ = 1.5406 Å). FT-IR spectra were collected from KBr pellets on an FTS-40 spectrophotometer. Thermogravimetric analysis (TGA)

was carried out under N_2 atmosphere on a NETZSCH STA 409 PC/PG instrument at a heating rate of 10 °C min^{-1}. Inductively coupled plasma mass spectrometry (ICP-MS) was performed on an X-Series II instrument. A Micromeritics ASAP 2020 surface area analyzer was used to measure N_2 gas adsorption/desorption isotherms. X-ray photoelectron spectra (XPS) were recorded on a VG ESCALAB MARK II machine. The conversion and chemoselectivity for the hydrogenation reaction were based on the GC-MS analysis results.

Catalytic hydrogenation of halogenated nitrobenzenes

Catalytic hydrogenation of halogenated nitrobenzene was performed in a 50 mL autoclave lined with polytetrafluoroethylene (PTFE). In a typical experiment, 0.5 mmol of halogenated nitrobenzene, PSM-11 (1.0 mol% based on Co and Ni), 1.5 mL of H_2O and 4.5 mL of ethanol were added into the autoclave. Hydrogen (1.0 MPa) was injected into the reactor three times to remove the dissolved air. The autoclave was heated at 130 °C in an oil bath for 1 h. The solid catalyst was separated by centrifugation, and the products were analyzed by GC-MS. The major products were calibrated by using standard curves.

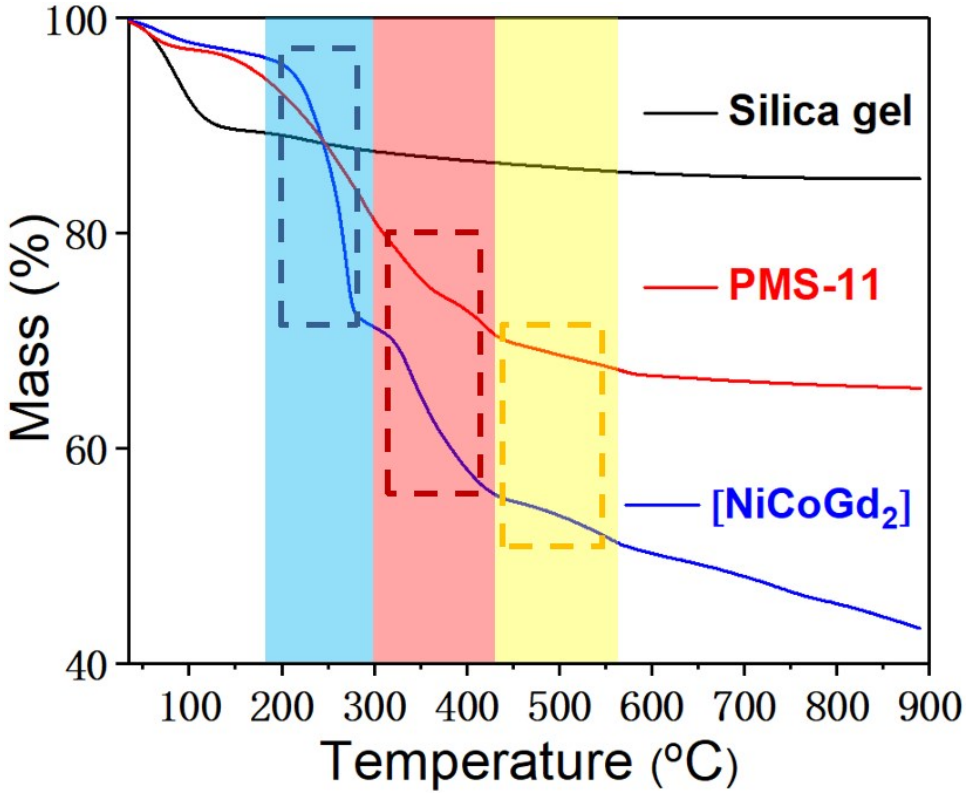

Fig. S1 TGA profiles for silica gel, [$NiCoGd_2$] and the PMS-11 precursor.

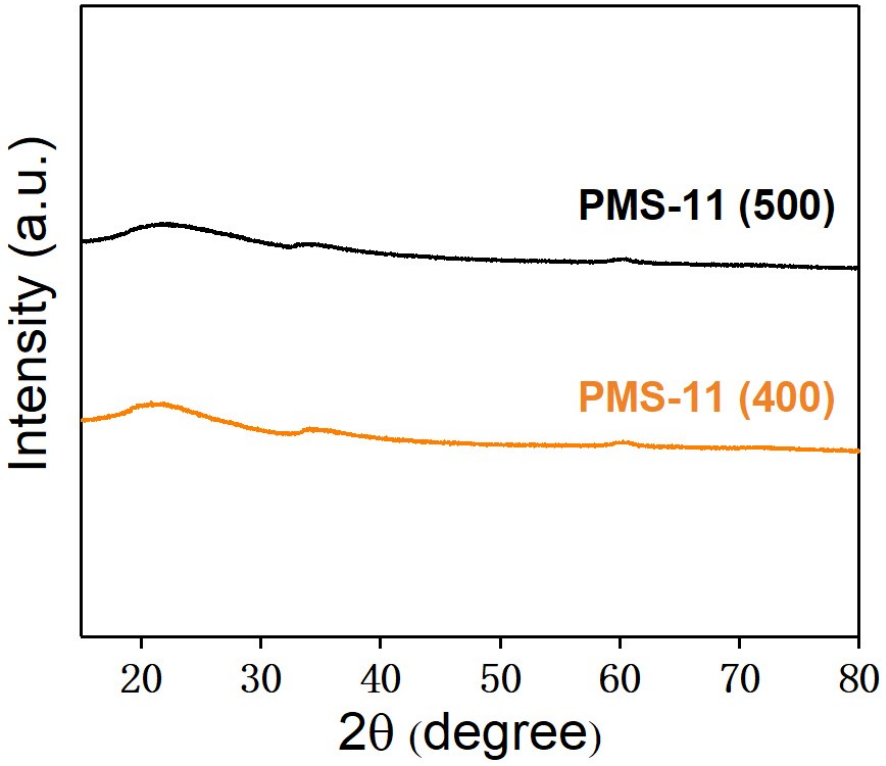

Fig. S2 PXRD profiles of PMS-11 (400) and PMS-11 (500).

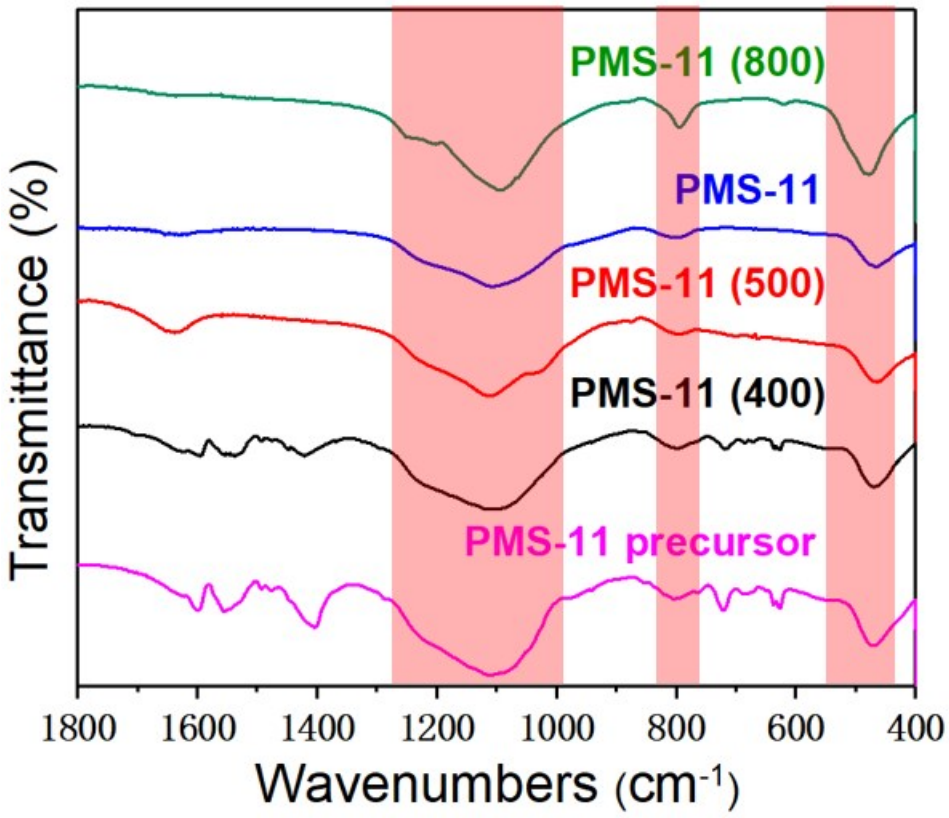

Fig. S3 FT-IR spectra of the PMS-11 precursor and its annealed products at different temperatures (the number in the parenthesis represents the annealing temperature).

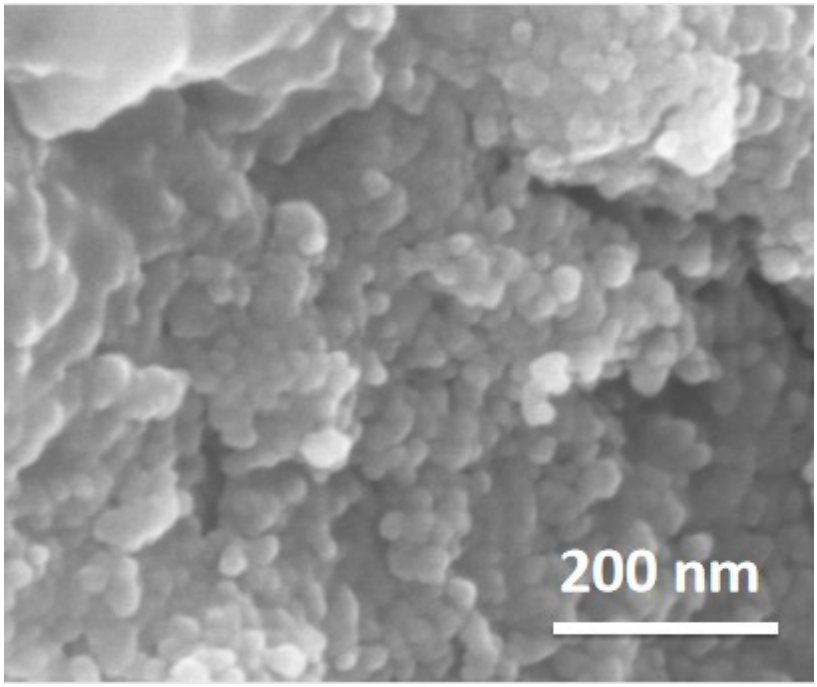

Fig. S4 SEM image of the PMS-11 precursor.

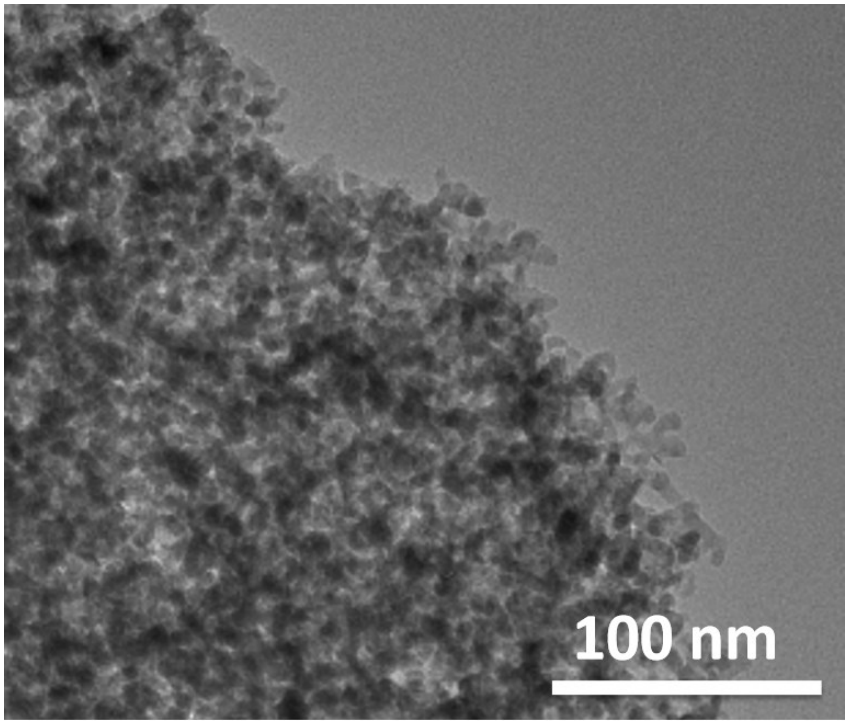

Fig. S5 TEM image of PMS-11.

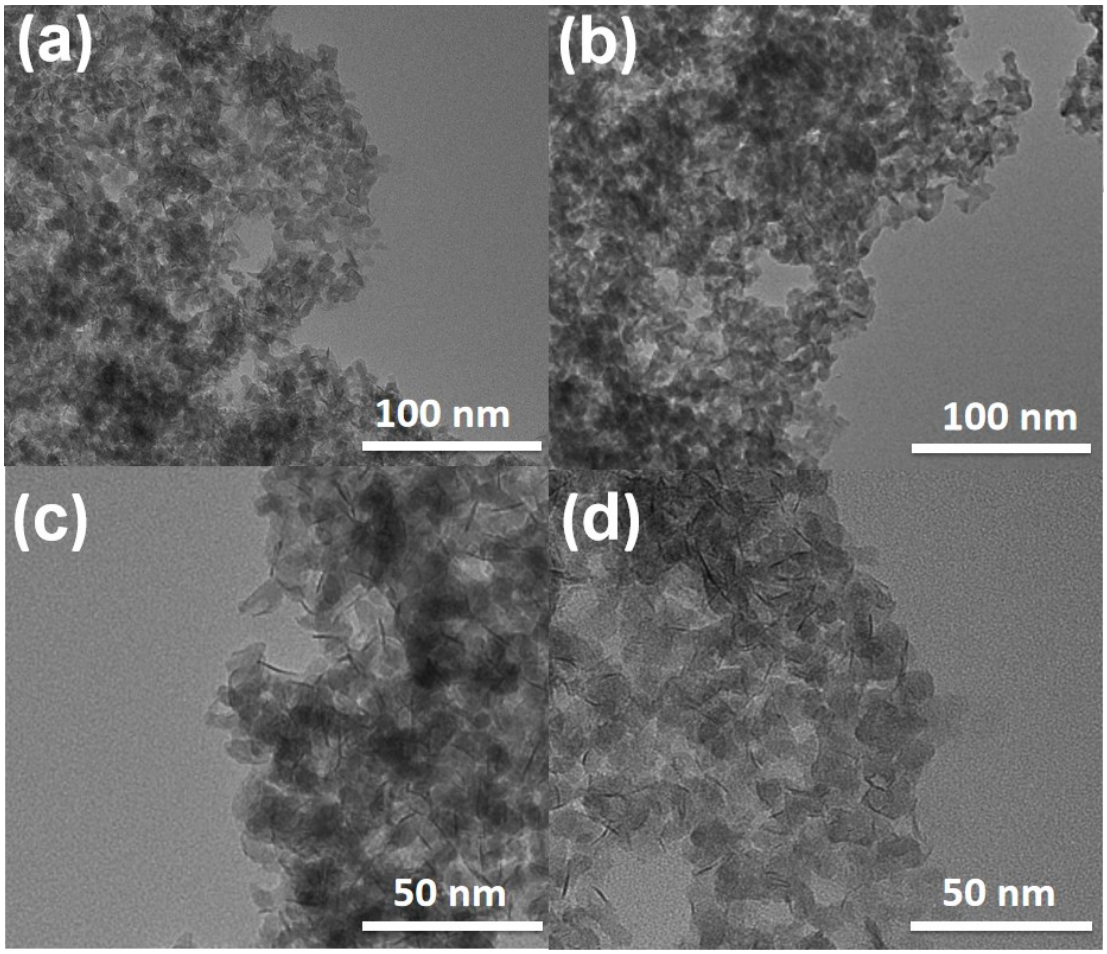

Fig. S6 TEM images of (a) PMS-11 (400), (b) PMS-11 (500), (c) PMS-11 (700) and (d) PMS-11 (800).

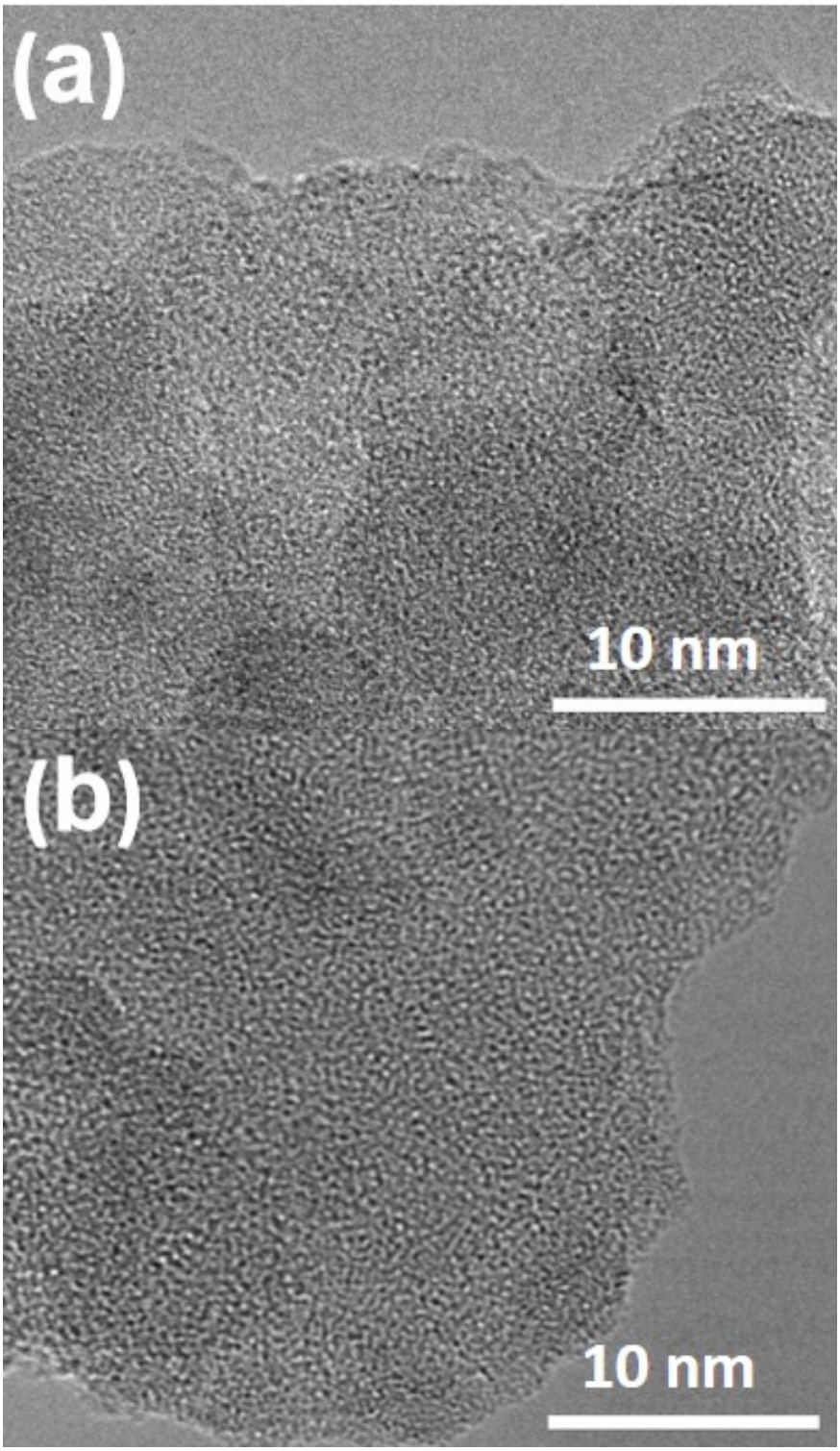

Fig. S7 HR-TEM images of (a) PMS-11 (400) and (b) PMS-11 (800).

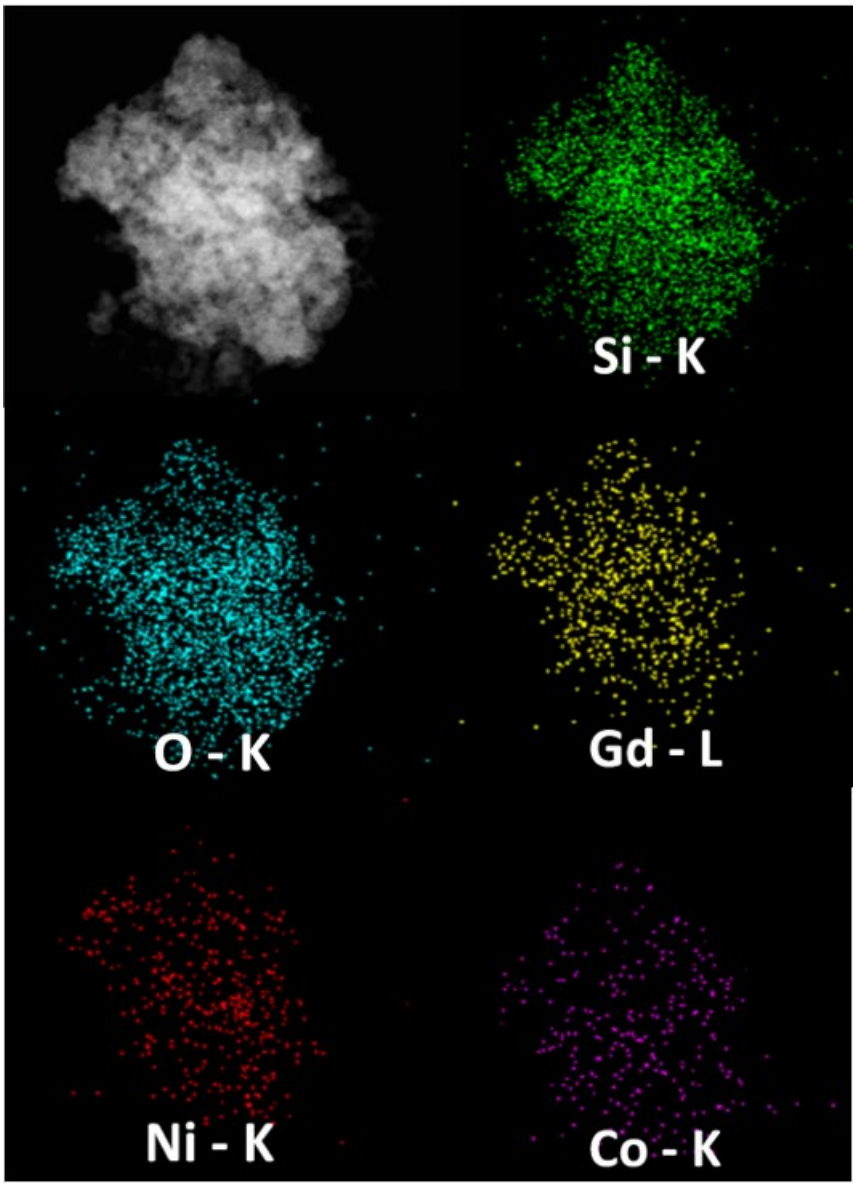

Fig. S8 STEM-EDS elemental mapping images for different elements in PMS-11.

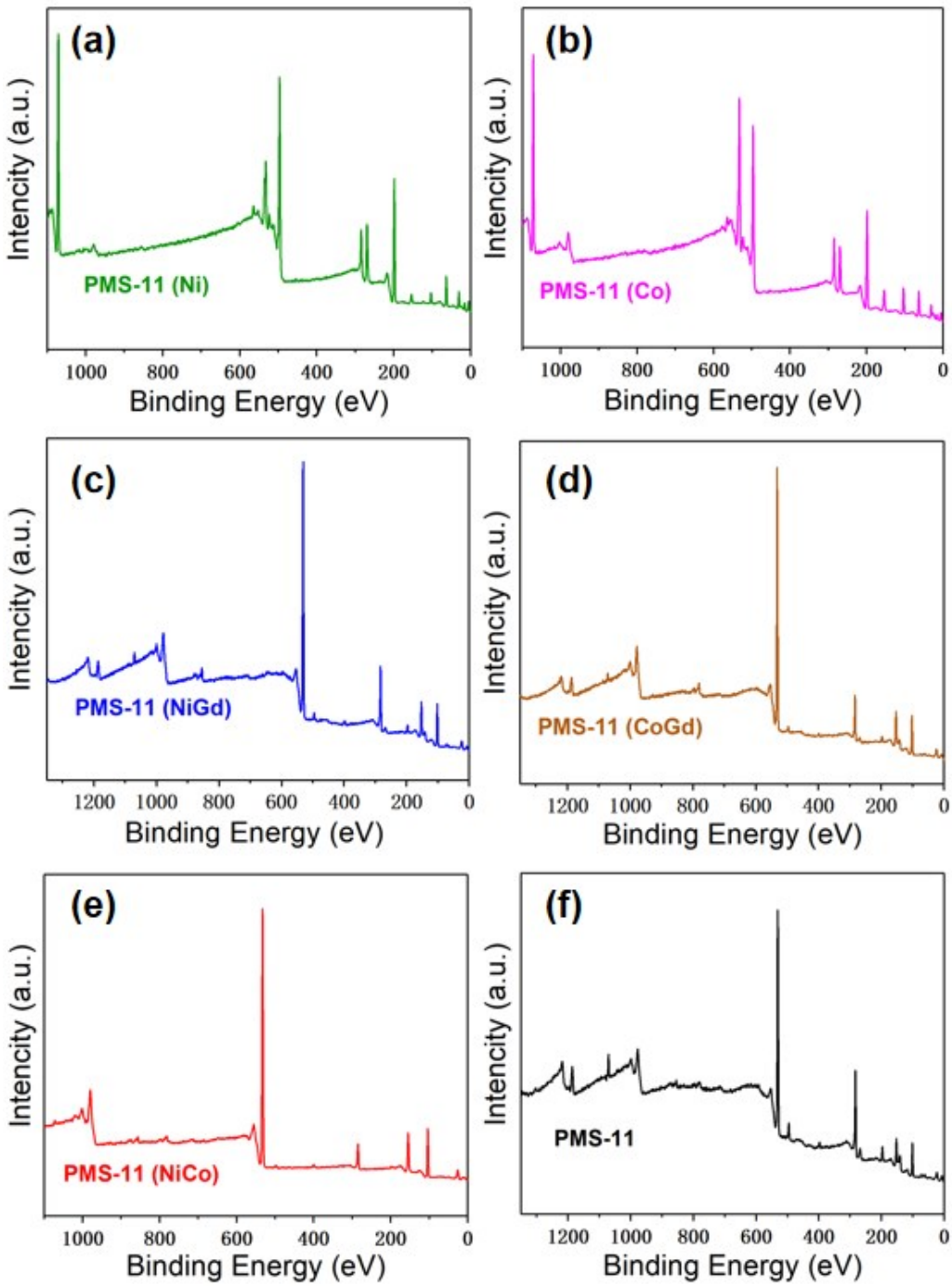

Fig. S9 XPS spectra of (a) PMS-11 (Ni), (b) PMS-11 (Co), (c) PMS-11 (NiGd), (d) PMS-11 (CoGd), (e) PMS-11 (NiCo) and (f) PMS-11.

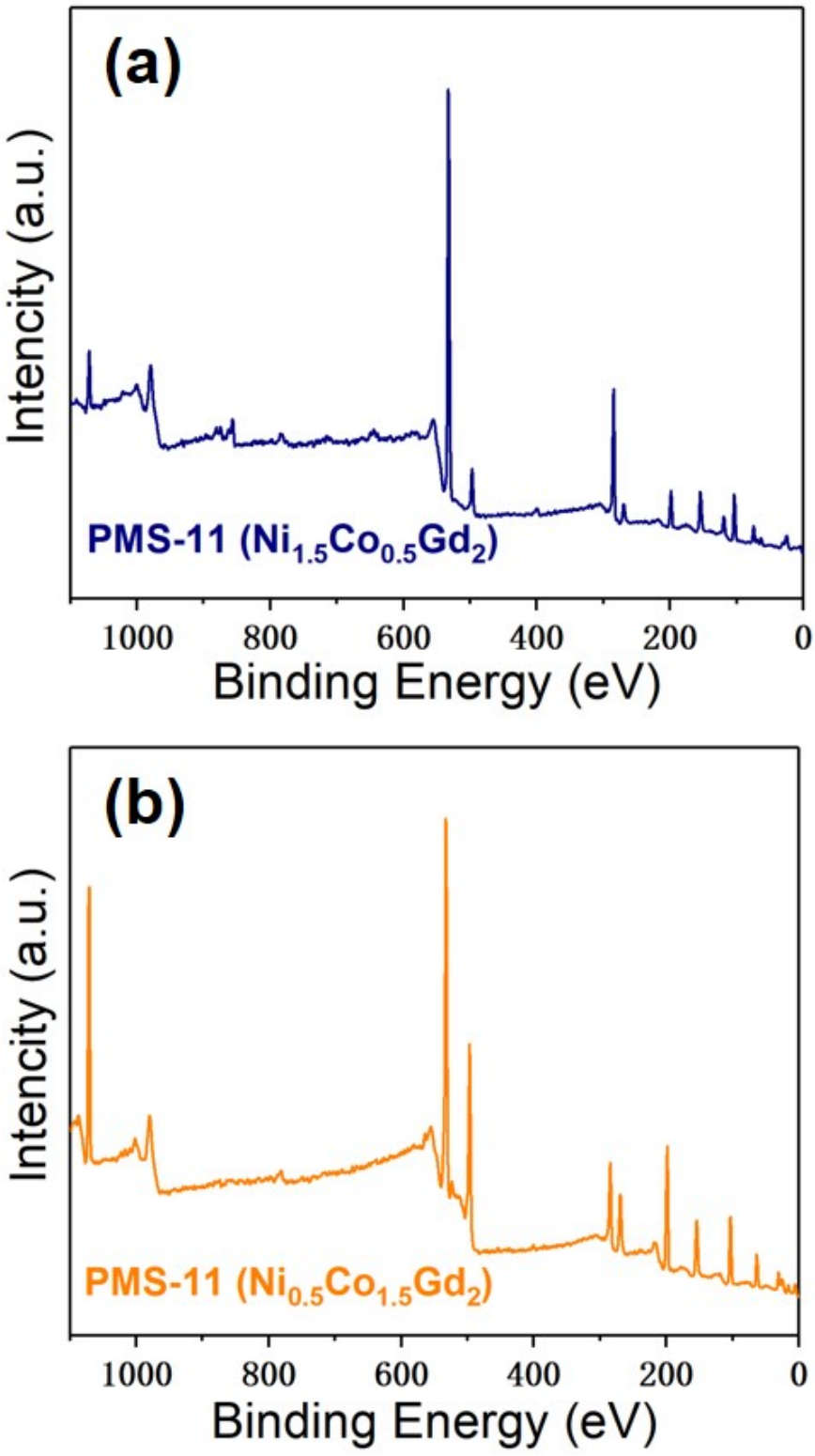

Fig. S10 XPS spectra of (a) PMS-11 ($Ni_{1.5}Co_{0.5}Gd_2$) and (b) PMS-11 ($Ni_{0.5}Co_{1.5}Gd_2$).

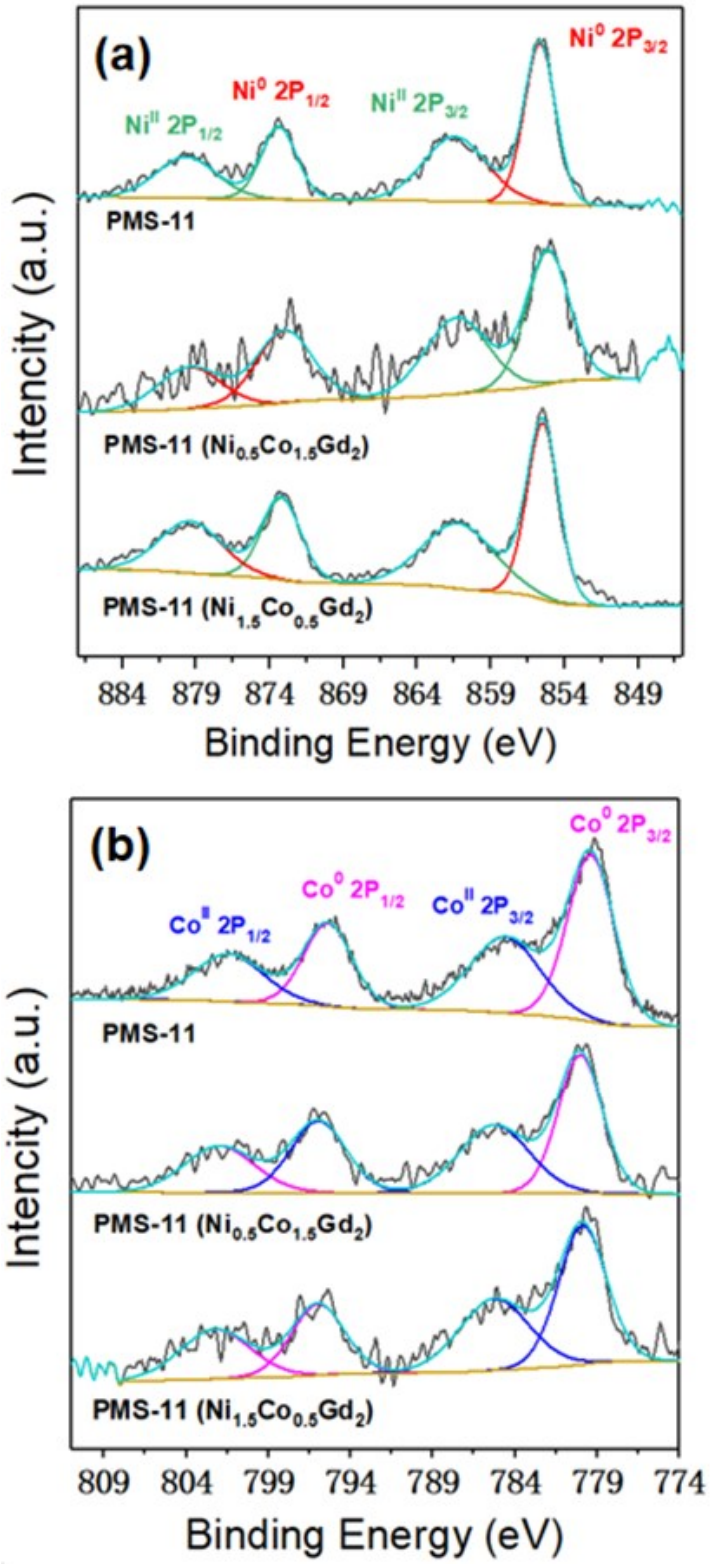

Fig. S11 (a) XPS Ni 2p spectra of PMS-11 ($Ni_{1.5}Co_{0.5}Gd_2$), PMS-11 ($Ni_{0.5}Co_{1.5}Gd_2$) and PMS-11. (b) XPS Co 2p spectra of PMS-11 ($Ni_{1.5}Co_{0.5}Gd_2$), PMS-11 ($Ni_{0.5}Co_{1.5}Gd_2$) and PMS-11.

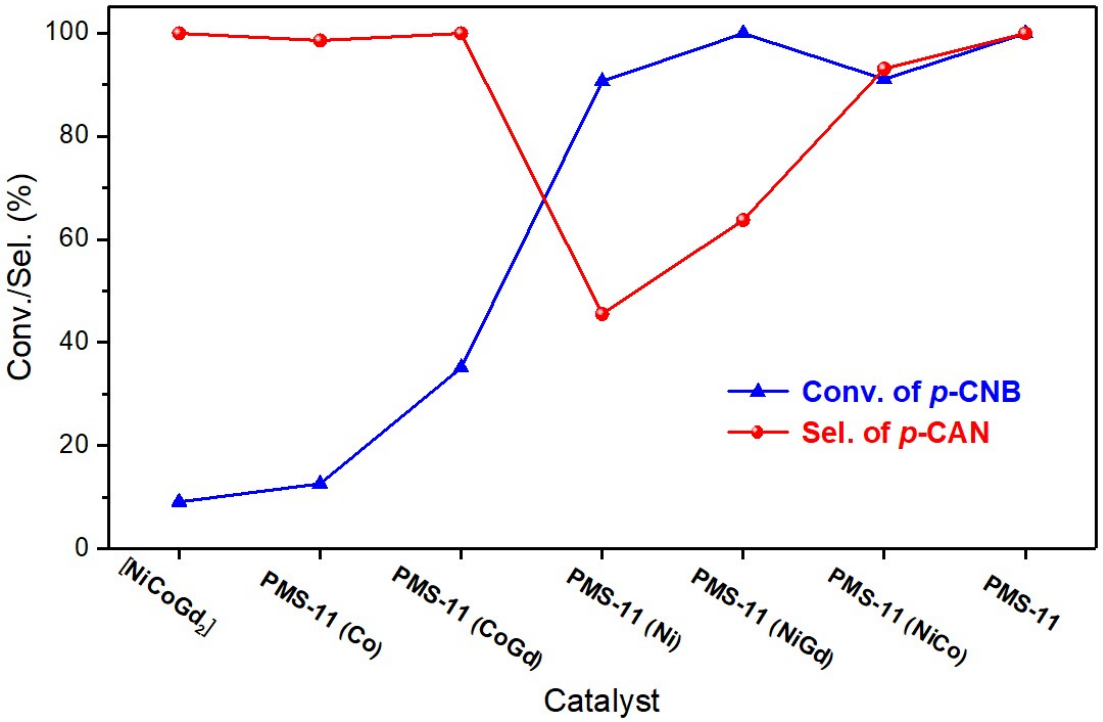

Fig. S12 Selective hydrogenation of *p*-CNB catalyzed by different catalysts. Reaction conditions: *p*-CNB (0.5 mmol), catalyst (1.0 mol% based on Ni and Co), H_2O (1.5 mL) and ethanol (4.5 mL), 1 h, 130 ^oC, 1 MPa H_2.

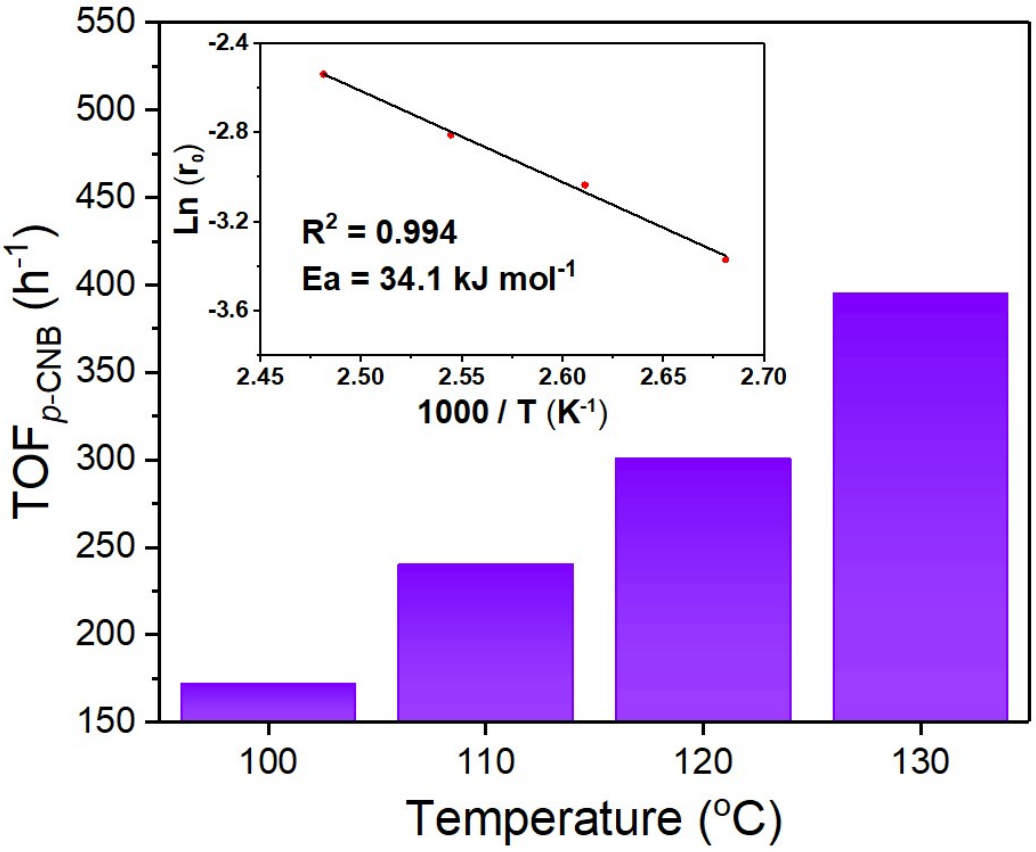

Fig. S13 Reaction rates for selective hydrogenation of *p*-CNB catalyzed by PMS-11 at different temperatures. Reaction conditions: *p*-CNB (5 mmol), PMS-11 (0.05 mol% based on Ni and Co), H_2O (2.5 mL) and ethanol (7.5 mL), 1 MPa H_2.

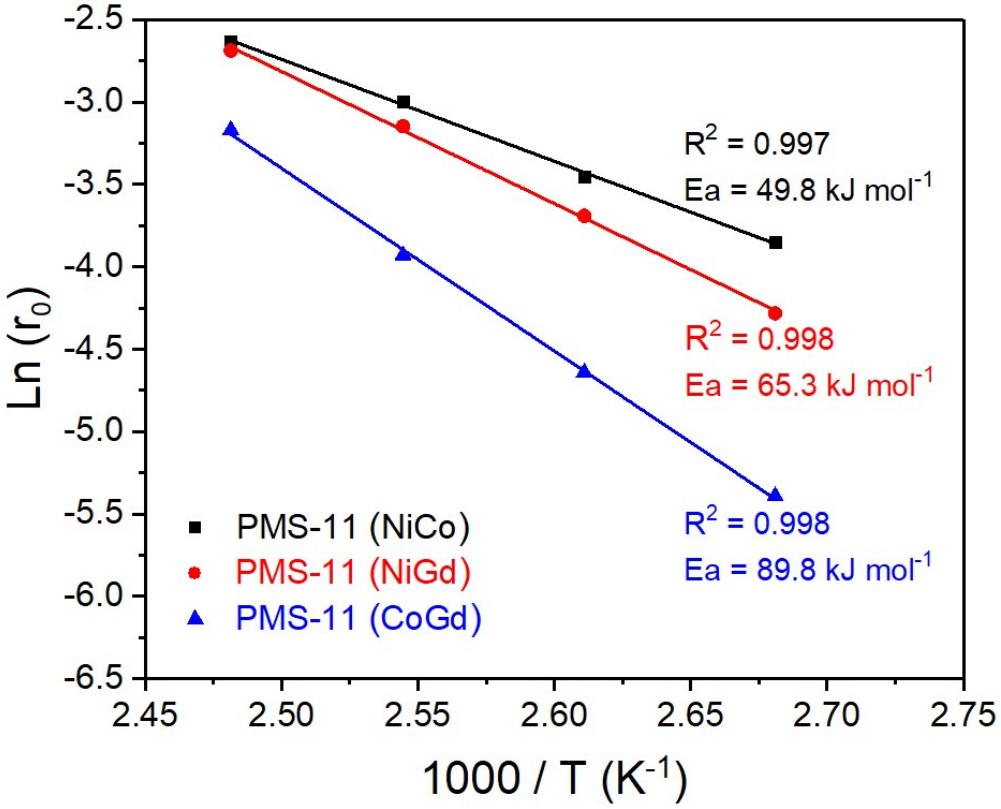

Fig. S14 Apparent activation energies (E_a) for selective hydrogenation of *p*-CNB catalyzed by PMS-11 (NiCo), PMS-11 (NiGd) and PMS-11 (CoGd).

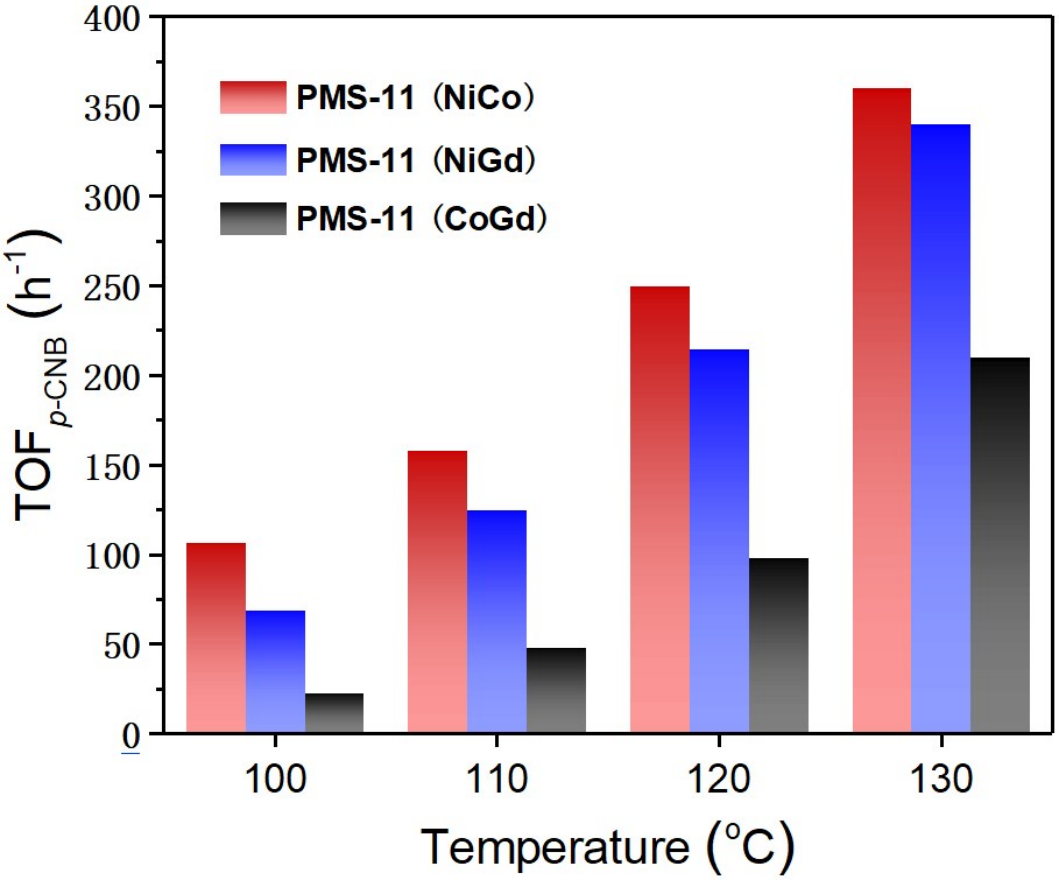

Fig. S15 Reaction rates for selective hydrogenation of *p*-CNB catalyzed by various catalysts at different temperatures. Reaction conditions: *p*-CNB (5 mmol), catalyst (0.04 mol% based on Ni and Co), H_2O (2.5 mL) and ethanol (7.5 mL), 1 MPa H_2.

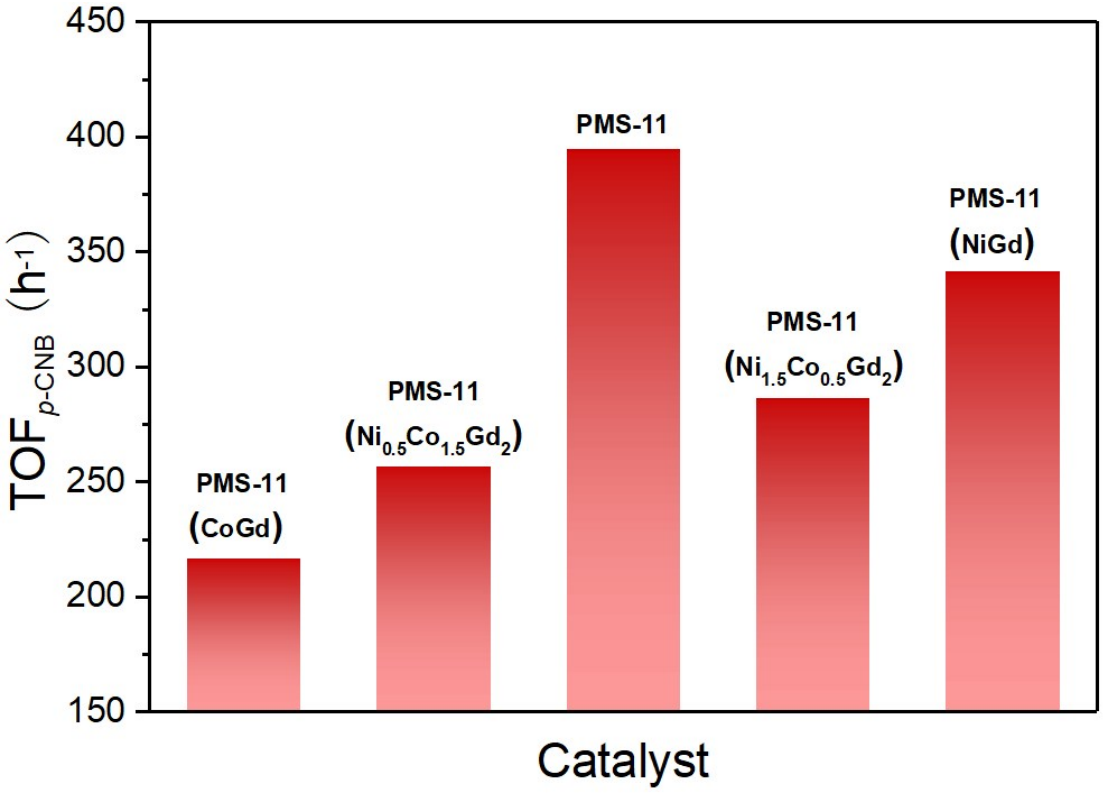

Fig. S16 The turnover frequencies (TOFs) for selective hydrogenation of *p*-CNB catalyzed by various catalysts with different Ni contents. Reaction conditions: *p*-CNB (5 mmol), catalyst (0.04 mol% based on Ni and Co), H_2O (2.5 mL) and ethanol (7.5 mL), 130 ^oC, 1 MPa H_2.

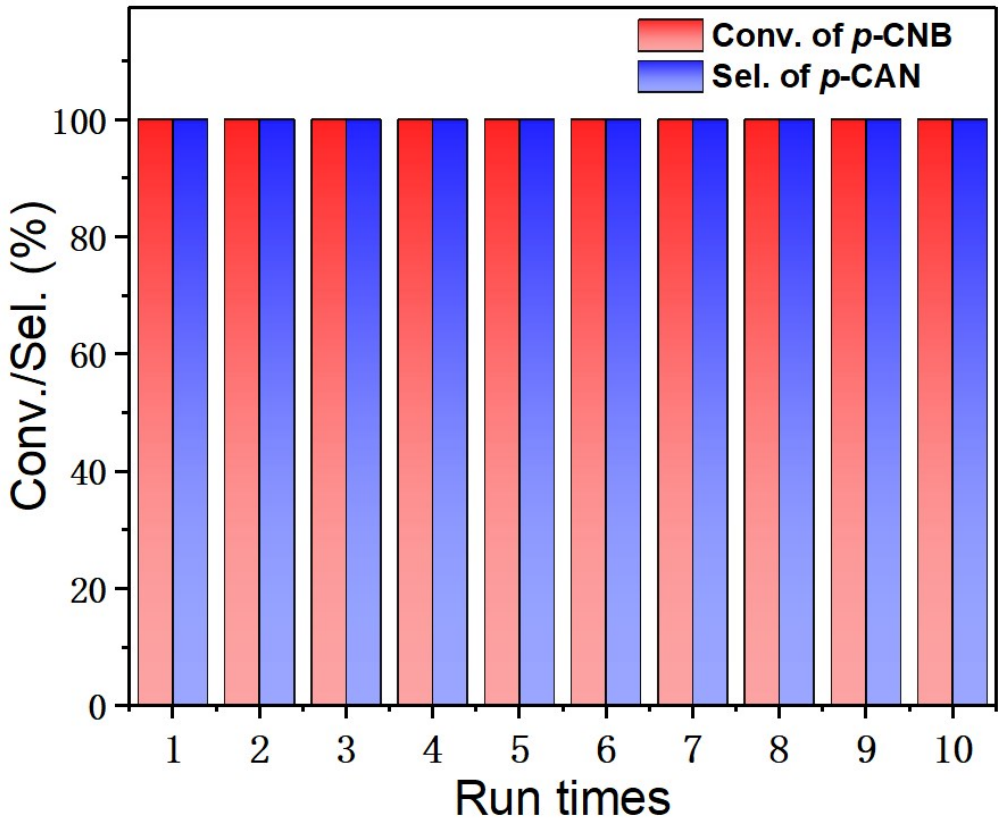

Fig. S17 Reusability test for PMS-11. Reaction conditions: *p*-CNB (0.5 mmol), PMS-11 (1.0 mol% based on Ni and Co), H_2O (1.5 mL) and ethanol (4.5 mL).

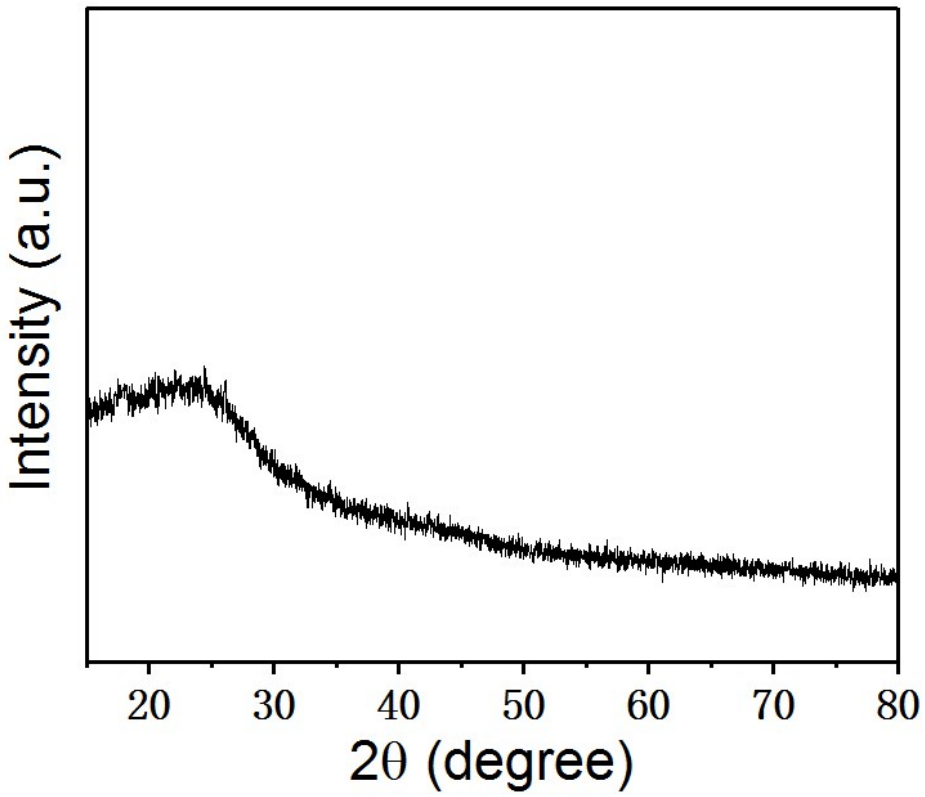

Fig. S18 PXRD profile of PMS-11 after catalysis.

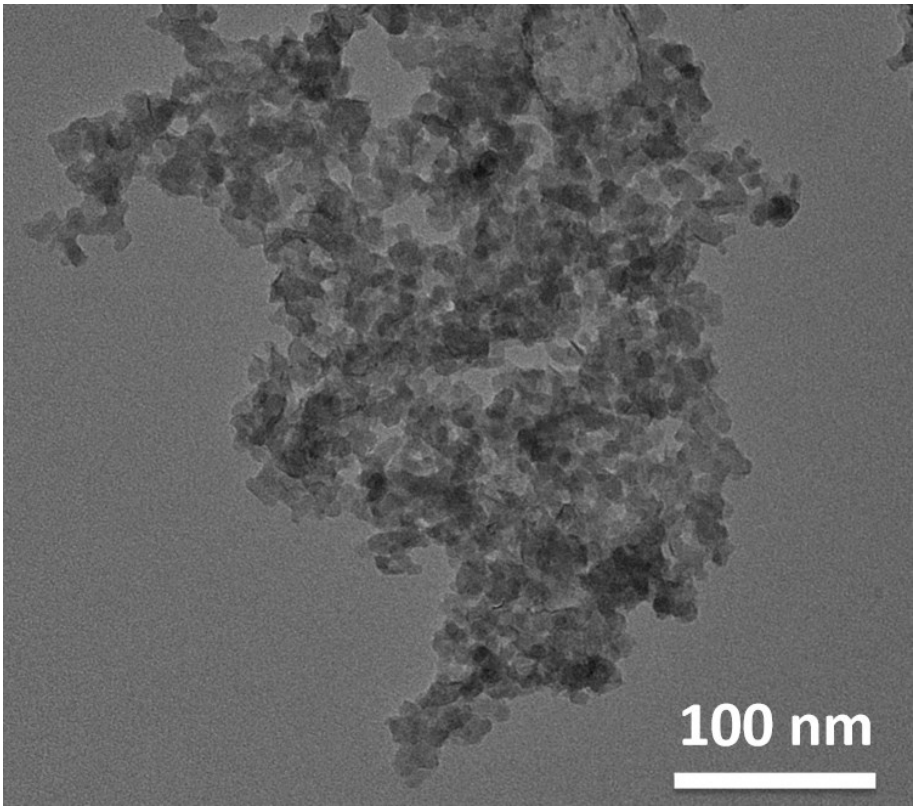

Fig. S19 TEM image of PMS-11 after catalysis.

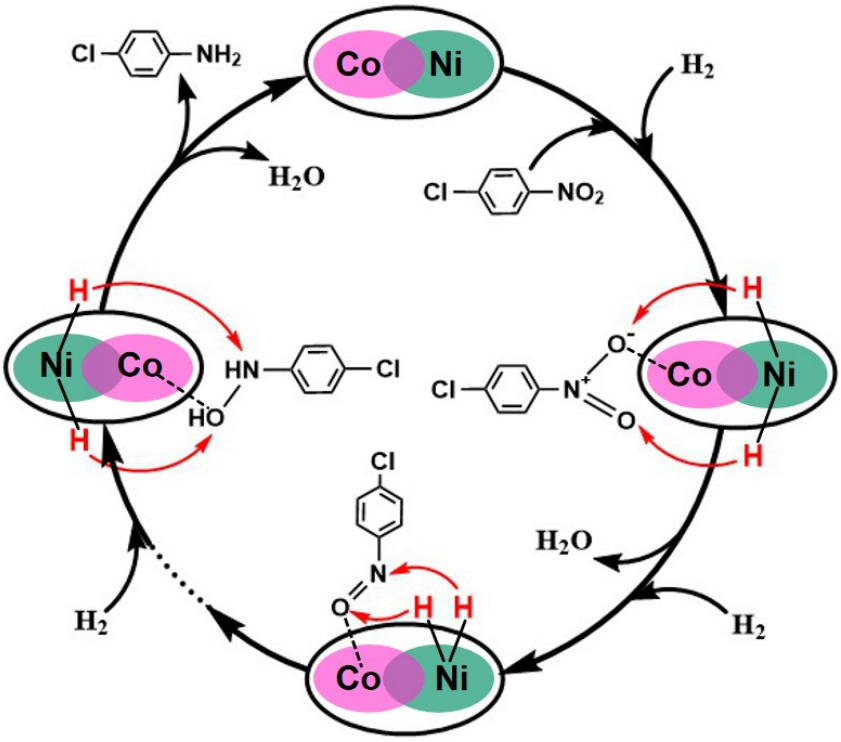

Scheme S1 A plausible catalytic mechanism for hydrogenation of *p*-CNB catalyzed by PMS-11.

Table S1. Textural properties of different materials

Material	Co (wt%)[a]	Ni (wt%)[a]	Gd (wt%)[a]	S_{BET} (m^2 g^{-1})[b]	Pore Size (nm)[b]
PMS-11 precursor	0.5	0.5	1.0	47	/
PMS-11	1.0	1.1	2.1	232	5

[a]Determined by ICP-MS. [b]Determined by multipoint BET method.

Table S2. Catalytic hydrogenation of *p*-CNB in different solvents by PMS-11[a]

Entry	Solvent	Time (h)	Conv. (%)[b]	Sel. (%)[b]
1	MeOH	1	43	>99
2	EtOH	1	62	>99
3	^{i}PrOH	1	81	>99
4	^{i}PrOH	2	>99	>99
5	^{i}PrOH+H_2O	1	>99	98.5
6	EtOH+H_2O	1	>99	>99

[a]Reaction conditions: *p*-CNB (0.5 mmol), PMS-11 (1.0 mol% based on Ni and Co), 130 ^{o}C, 1 MPa H_2. [b]Determined by GC-MS.

Table S3. Selective hydrogenation of *p*-CNB by various control catalysts[a]

Entry	Catalyst (annealing temperature)	Conv. (%)[b]	Sel. (%)[b]
1	PMS-11 (400)	0.4	>99
2	PMS-11 (500)	0.7	>99
4	PMS-11 (700)	4.3	93.5
5	PMS-11 (800)	3.3	16.7
6	PMS-11 ($Ni_{1.5}Co_{0.5}Gd_2$) (600)	65.7	>99
7	PMS-11 ($Ni_{0.5}Co_{1.5}Gd_2$) (600)	51.6	>99

[a]Reaction conditions: *p*-CNB (0.5 mmol), PMS-11 (1.0 mol% based on Ni and Co), H_2O (1.5 mL) and ethanol (4.5 mL), 130 ^oC, 1 MPa H_2, 1 h. [b]Determined by GC-MS.

Table S4. Comparison of the catalytic performances of different noble metal-based catalysts in catalytic hydrogenation of *p*-CNB to produce *p*-CAN

Catalyst	T (^oC)	H_2 (MPa)	t (h)	Conv. (%)	Sel. (%)	Ref.
Ag/SiO_2-200	140	2.0	3	100	100	S1
0.12Pd–Si	100	1.0	36	>99.9	>99.9	S2
Pd–NiO@SiO_2	30	0.1	2.5	100	82.7	S3
Pd@Pt-1/0.25/Al_2O_3	45	0.1	3	98.5	82.1	S4
5 wt% Pt/CMK-3	25	4.0	0.17	77.7	>99	S5
Ru5/NPC(NB)	140	1.5	2.5	98	98	S6
Ag/C60 NCC	140	3.0	3	>99	>99	S7
PMS-11	130	1.0	1	>99	>99	This work

Table S5. Comparison of the catalytic performances of different non-noble metal-based catalysts in catalytic hydrogenation of *p*-CNB to produce *p*-CAN

Catalyst	T (°C)	H_2 (MPa)	t (h)	Conv. (%)	Sel. (%)	Ref.
Co-B/CNTs	140	3.0	3	96.2	93.4	S8
Co@mesoNC	110	3.0	2	73	>99	S9
$Co_{50}Ni_{50}$/C	140	2.0	2	99.8	98	S10
Ni/TiO_2@OAC	70	2.0	7	100	98	S11
CN/Ni/Al2O3	120	1.0	10	96.8	>99.9	S12
12%Ni/Al-SBA-15	110	2.5	7.5	100	95	S13
Co@C NPs	140	1.0	8	99	97	S14
Co@CN-400	60	1.0	1.5	100	>99	S15
CN1meso-Co	100	1.5	14	100	100	S16
2-NiC-Ni/CNFs	140	2.0	2.5	>99	>99	S17
Co^0/Co_3O_4@ NCNTs	110	3.0	3	>99	>99	S18
Co oxide-N/C	110	5.0	6	>99	95	S19
Fe-phen/C-800	120	5.0	12	96	98	S20
PMS-11	130	1.0	1	>99	>99	This work

Table S6. Selective hydrogenation of *o*-iodonitrobenzene catalyzed by different control catalysts[a]

Entry	Catalyst	Conv. (%)[b]	Sel. (%)[b]
1	[Ni]	5.5	74
2	[Co]	1.7	>99
3	[Ni]+[Co]	7.1	85
4	[NiCo]	8.2	93
5	[NiGd]	6.1	86
6	[CoGd]	2.0	>99
7	[NiGd] + [CoGd]	7.8	94
8	[$NiCoGd_2$]	8.5	>99

[a]Reaction conditions: *o*-iodonitrobenzene (0.5 mmol), catalyst (1.0 mol% based on Ni and Co), H_2O (1.5 mL) and ethanol (4.5 mL), 130 ^oC, 1 MPa H_2, 4 h. [b]Determined by GC-MS.

References

S1 Y. Chen, C. Wang, H. Liu, J. Qiu and X. Bao, *Chem. Commun*., 2005, **42**, 5298-300.

S2 Q. Wei, Y. S. Shi, K. Q. Sun and B. Q. Xu, *Chem. Commun*., 2016, **52**, 3026-3029.

S3 H. Liu, K. Tao, C. Xiong and S. Zhou, *Catal. Sci. Technol*., 2015, **5**, 405-414.

S4 P. Zhang, Y. Hu, B. Li, Q. Zhang, C. Zhou, H. Yu, X. Zhang, L. Chen, B. Eichhorn and S. Zhou, *ACS Catal*., 2015, **5**, 1335-1343.

S5 J. Li, X. Li, Y. Ding and P. Wu, *Chin. J. Catal*., 2015, **36**, 1995-2003.

S6 X. Li, S. Zhao, W. Zhang, Y. Liu and R. Li, *Dalton Trans*., 2016, **45**, 15595-15602.

S7 B. Li, H. Li and Z. Xu, *J. Phys. Chem. C*, 2009, **113**, 21526-21530.

S8 F. Li, *Appl. Catal. A: Gen*., 2016, **514**, 248-252.

S9 X. Sun, A. I. Olivos-Suarez, D. Osadchii, M. J. Valero Romero, F. Kapteijn and J. Gascon, *J. Catal*., 2018, **357**, 20-28.

S10 Y. L. Xie, N. Xiao and Z. Ling, *Chin. J. Catal*., 2012, **33**, 1883-1888.

S11 L. Huang, Y. Lv and S. H. Liu, *Ind. Eng. Chem. Res*., 2020, **59**, 1422-1435.

S12 T. Fu, P. Hu, T. Wang, Z. Dong, N. Xue, L. Peng, X. Guo and W. Ding, *Chin. J. Catal*., 2015, **36**, 2030-2035.

S13 R. Ren and J. Ma, *RSC Adv*., 2015, **5**, 74802-74810.

S14 L. Liu and P. Concepción, A. Corma, *J. Catal.*, 2016, **340**, 1-9.

S15 Y. Cao, K. Liu, C. Wu, H. Zhang and Q. Zhang, *Appl. Catal. A: Gen*., 2020, **592**, 117434.

S16 R. L. Oliveira, M. C. Ben Ghorbel, S. Praetz, D. Meiling, C. Schlesiger, R. Schomacker and A. Thomas, *ACS Sustain. Chem. Eng.*, 2020, **8**, 11171-11182.

S17 J. Kang, R. Han, J. Wang, L. Yang, G. Fan and F. Li, *Chem. Eng. J.*, 2015, **275**, 36-44.

S18 Z. Wei, J. Wang, S. Mao, D. Su, H. Jin, Y. Wang, F. Xu, H. Li and Y. Wang, *ACS Catal.*, 2015, **5**, 4783-4789.

S19 F. A. Westerhaus, R. V. Jagadeesh, G. Wienhöfer, M.-M. Pohl, J. Radnik, A.-E. Surkus, J. Rabeah, K. Junge, H. Junge, M. Nielsen, A. Brückner and M. Beller, *Nat. Chem.*, 2013, **5**, 537-543.

S20 R. V. Jagadeesh, A.-E. Surkus, H. Junge, M.-M. Pohl, J. Radnik, J. Rabeah, H. Huan, V. Schünemann, A. Brückner and M. Beller, *Science*, 2013, **342**, 1073-1076.